Manh Tung Ngo[1,2],
Quang Dich Nguyen[2],
Tung Lam Nguyen[2*]

Speed Sensorless Control of PMSM–Magnetic Bearing Systems Using High-Gain Observer

Permanent synchronous motor (PMSM) drive systems incorporates magnetic bearings performing speed control and rotor balancing control between the two stators simultaneously. This paper deals with adjusting the motor speed based on the stator current components measurement. The back electromotive force (back-EMF) generated in the stator is estimated by a high-gain observer. A rotor angular position and velocity are calculated through α-β components of the back-EMF. A motor drive is built in a vector control structure based on the rotor flux, using PID controllers to control rotor position and speed. A speed feedback signal is taken from the output of the High-Gain observer. Simulation results on Matlab-Simulink software show that the output speed value follows the set trajectory, and the rotor is controlled in the equilibrium position. This mean that the High-Gain Observer has good estimations.

Keywords: PMSM; magnetic self-bearing motor; back- EMF; high-gain observer.

1. Introduction

In recent years, the motor of integrated magnetic bearing has been paid more attention due to its advantages compared to traditional mechanical bearing [1]. The motor studied in this paper is a synchronous motor with a permanent magnet attached to the rotor and two stators with winding on either side of the rotor. Assuming that the motor shaft is raised steadily by horizontal drive bearings, the object then has two degrees of freedom, namely rotational motion and position displacement along the rotor shaft [2]-[3].

Mathematical model of the synchronous motor integrating magnetic bearings (PMSM-AMB) exhibits nonlinearities and complex controls. Because air gap in conventional motors is usually constant, while the PMSM-AMB has a rotor move with two degrees of freedom. So the position of the rotor angle and the air gap between the stator and the rotor continuously change acting to the motor parameters. Besides the control process needs to split the channel between the torque that creates the rotation and the force acting along axial axis. Therefore, in this paper, the vector control structure based on the rotor magnetic flux is proposed, can solve the above problems. However, the system is necessary to perform coordinate transformation [4]. The transformation requires accurate information about the rotor angular position. The rotor data normally acquired through the rotation angle sensor and speed feedback signal is also taken from this sensor. The utilization of the sensor increases the total investment cost, increases size and reduces system reliability. Therefore, several methods of replacing speed measuring sensors with computational techniques have been developed [5]-[7].

In published works on control not measuring rotational speed for synchronous motors, two approaches can be used to estimate the angular position and rotor speed.

*Corresponding author: Tung Lam Nguyen, E-mail: lam.nguyentung@hust.edu.vn
[1]Faculty of Electrical Engineering, Hanoi University of Industry, Ha Noi, Viet Nam.
[2]School of Electrical Engineering, Hanoi University of Science and Technology, Ha Noi, Viet Nam.

The first direction is based on the inductance variation due to the extreme protrusion on the *d-q* axes [8]-[10],[11]-[14]. Inductance difference is used to directly estimate rotor position. The rotor inductance can be considered as a function of the rotor position, so the rotor position information will be obtained from the constant updating of the inductance on the stator. This method is applicable to the kinetic process at low speed range and nearly stop. The second approach is based on estimating the back-EMF electromotive force, which combines the stator and current measurement [3],[5],[15]-[18]. From the back-EMF value, we can estimate rotor angle position and calculate the rotation speed. The drawback of this method is that the back-EMF components are too small and sensitive to disturbance and variable motor parameters, so it is difficult to apply at low speed range and nearly stop. However, the advantage is reduced computing volume, simplicity, ease of design and installation in the drive system.

This paper presents a High-Gain (HG) observer is designed according to the second approach [19]-[20] for PMSM-AMB. A vector control structure transformation sis proposed, in which the HG observer estimates the value of the back-EMF from the stator current measurement and the reference voltage value, thereby calculating the angular position rotor and rotation speed. The feasibility of the method is demonstrated through simulation results.

2. Motor mathematical model

The structure of the permanent excitation synchronous motor integrated with the magnetic bearing is shown in Figure 1. The rotor is lifted by two horizontal magnetic bearings. The movement in the *x*, *y*, θ_x, and θ_y directions of the rotor is assumed to depend only on the drive control of axial magnetic bearings. The scope of the paper only pays attention to the rotation and translational movement along the *z* axis, so the motor consists of two degrees of freedom. Rotor is a flat disc with permanent magnets attached to the rotor surface (nonsalient-pole rotor) or mounted in the rotor surface (salient-pole rotor). Each side of the rotor is a stator, on which each stator consists of three three-phase coils that create a rotating magnetic field in the air gap. This magnetic field generates torque of T_1 and T_2 on the rotor and the suction forces F_1 and F_2 between the rotor and each stator. Total torque *T* is calculated as the addition of two component moments. The axial force *F* is calculated as the difference of the two axial forces [1].

The mathematical model of the motor is presented on the axis system based on the rotor flux (*d*, *q*) or the stator generator (*α*, *β*). Calculating axial force and torque for a stator and then summing up to have a general mathematical model for the engine.
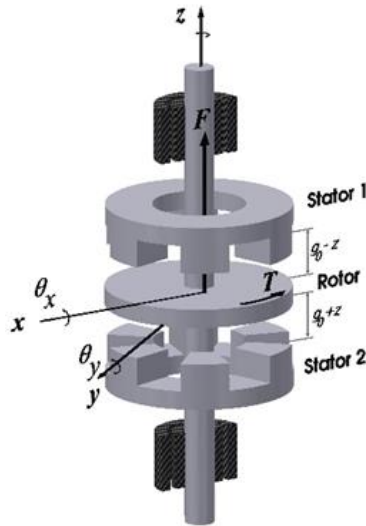
Fig. 1. Structure of the permanent excitation synchronous motor integrated with the magnetic bearing [1]

If the rotor is a salient-pole rotor, the inductance on the stator will depend on the position of the rotor angle and on the air gap between the stator and the rotor. If the rotor is a nonsalient-pole rotor, the inductance does not depend on the rotor angle position and the value on the d and q axis can be considered approximately equal. Often this inductance will be inversely proportional to the clearances, so we have the following approximate formula [1], [2]:

$$L_s = \frac{3}{2} \frac{L'_{s0}}{g} + L'_{sl} \tag{1}$$

And mutual inductance: $L_m = \frac{3}{2} \frac{L'_{s0}}{g}$ $\tag{2}$

For L'_{s0}: inductance per gap unit; L_{sl}: leakage inductance; $g = g0 \pm z$: clearance between stator and rotor; $g0$: clearance at equilibrium position; z: displacement from the equilibrium position. Equation of the vector voltage of a stator on the $\alpha\beta$ coordinate system:

$$U_s = i_s R_s + L_s \frac{di_s}{dt} + e_s \tag{3}$$

With i_s the stator line vector, U_s is the stator voltage vector. Vector e_s electromotive induction:

$$e_s = \frac{d\lambda_m}{dt} = \omega_e \frac{d\lambda_m}{d\theta_e} \tag{4}$$

Where λ_m is the flux linkage between the rotor and the stator. e_s is the sine function and represents the components on the $\alpha\beta$ coordinate system as follows:

$$\begin{cases} e_{s\alpha} = -\left|\lambda_m\right|\omega_e \sin\theta_e \\ e_{s\beta} = \left|\lambda_m\right|\omega_e \cos\theta_e \end{cases} \tag{5}$$

Where ω_e is the rotor speed, θ_e is the position of the rotor flux vector. From (3) we have:

$$\begin{cases} \dfrac{di_{s\alpha}}{dt} = -\dfrac{R_s}{L_s}i_{s\alpha} + \dfrac{1}{L_s}u_{s\alpha} - \dfrac{1}{L_s}e_{s\alpha} \\ \dfrac{di_{s\beta}}{dt} = -\dfrac{R_s}{L_s}i_{s\beta} + \dfrac{1}{L_s}u_{s\beta} - \dfrac{1}{L_s}e_{s\beta} \end{cases} \tag{6}$$

From the above equations, it is possible to calculate the back-EMF value if the current and voltage information is known, the rotor position and speed can be calculated. From [1]-[3] control system principles:

$$\begin{cases} i_{q1} = i_{q2} = i_q \\ i_{d1} = i_{d0} - i_d \\ i_{d2} = i_{d0} + i_d \end{cases} \tag{7}$$

In which i_{d1} and i_{d2} are components of the axial current on two stators generating axial force F_1 and F_2; i_{d0} is the offset line and has a very small value or approximate zero. If the displacement is zero or very small compared to the air gap at the equilibrium point g_0 we have:

$$F = 4K_{Fd}i_f i_d \tag{8}$$

$$T = 2K_T i_q \tag{9}$$

With $K_{Fd} = -3L_{sd0}'/4g_0^2$ is the axial coefficient; $K_T = -3PL_{sd0}'i_f/2g_0$ is the torque coefficient.

Fig. 2. Control structure does not measure motor rotation speed

The control structure does not use a speed sensor for the synchronous motor incorporating a magnetic bearing using the HG observer as shown in Figure 2. This structure is based on the vector control principle based on the rotor flux on *dq* coordinate, with the *d*-axis coinciding with the rotor flux vector [4],[5]. The rotor speed calculated by the observer is compared with the reference speed value, then the deviation is fed into the speed regulator R_ω.

The current on the two phases of the stator on the *αβ* coordinate system is obtained by measuring the current on the two real phases. The current components on the *dq* coordinate system are then calculated based on the rotor position taken from the monitor. The *q*-axis components are controlled by the reference values taken from the speed controller, while the *d*-axis components are controlled by the reference values taken from the axial position controller. The output of the current controller is used to calculate reference voltage values. We need to use the transfer of the rotating coordinate system to the three-phase stator fixed reference system. The motor direct current for stator phases is supplied from PWM pulse width modulators. The speed controller is PI, the position controller is PID. Design procedure of position and speed controller can be found in [2]-[3].

3. High-gain observer design

The HG observer's task is to estimate the values of $e_{s\alpha}$ and $e_{s\beta}$ components of the back-EMF quickly follow the true value of the back-EMF of the motor, thereby calculating the value of the rotor angle Θ converges fast enough. The input of the HG observer i_s the stator current component and the u_s reference voltage on the *α-β* coordinate system. From (5) and (6) we have:

$$e_{s\alpha} = -|\lambda_m|\omega_e \sin\theta_e = \underbrace{-L_{s\alpha}\frac{di_{s\alpha}}{dt} - R_s i_{s\alpha} + u_{s\alpha}}_{h_\alpha}$$

$$e_{s\beta} = |\lambda_m|\omega_e \cos\theta_e = \underbrace{-L_{s\beta}\frac{di_{s\beta}}{dt} - R_s i_{s\beta} + u_{s\beta}}_{h_\beta} \tag{10}$$

The back-EMF values estimated from the observer are denoted $\hat{e}_{s\alpha}$ and $\hat{e}_{s\beta}$. The high gain estimation is expressed as:

$$\dot{\hat{e}}_{s\alpha} = \frac{1}{\varepsilon_\alpha}(-L_{s\alpha}\frac{di_{s\alpha}}{dt} - R_s i_{s\alpha} + u_{s\alpha} - \hat{e}_{s\alpha})$$

$$= -\frac{1}{\varepsilon_\alpha}\hat{e}_{s\alpha} + \frac{1}{\varepsilon_\alpha}h_\alpha$$

$$\dot{\hat{e}}_{s\beta} = \frac{1}{\varepsilon_\beta}(-L_{s\beta}\frac{di_{s\beta}}{dt} - R_s i_{s\beta} + u_{s\beta} - \hat{e}_{s\beta}) \tag{11}$$

$$= -\frac{1}{\varepsilon_\beta}\hat{e}_{s\beta} + \frac{1}{\varepsilon_\beta}h_\beta$$

where ε_α and ε_β are the factors of the HG observation. From (10) and (11), state space representation of the system is formulated as:

$$\dot{x} = Ax + Bu + H$$
$$y = Cx \tag{12}$$

Where $x = [i_{s\alpha} \;\; i_{s\beta} \;\; \hat{e}_{s\alpha} \;\; \hat{e}_{s\beta}]^T$ is the state vector of the observation, $u = [u_{s\alpha} \;\; u_{s\beta}]^T$ is the input vector of the observation,

$y = [i_{s\alpha} \;\; i_{s\beta} \;\; \hat{e}_{s\alpha} \;\; \hat{e}_{s\beta}]^T$ is the output vector of the observation.

$$A = \begin{bmatrix} -R_s/L_{s\alpha} & 0 & -1/L_{s\alpha} & 0 \\ 0 & -R_s/L_{s\beta} & 0 & -1/L_{s\beta} \\ 0 & 0 & -1/\varepsilon_\alpha & 0 \\ 0 & 0 & 0 & -1/\varepsilon_\beta \end{bmatrix} \text{ is the system matrix; } B = \begin{bmatrix} 1/L_{s\alpha} & 0 \\ 0 & 1/L_\beta \\ 0 & 0 \\ 0 & 0 \end{bmatrix} \text{ is}$$

the input matrix. (13)

$$C = \begin{bmatrix} 1 & 0 & 0 & 0 \\ 0 & 1 & 0 & 0 \\ 0 & 0 & 1 & 0 \\ 0 & 0 & 0 & 1 \end{bmatrix} \text{ is the output matrix; } H = \begin{bmatrix} 0 \\ 0 \\ h_\alpha / \varepsilon_\alpha \\ h_\beta / \varepsilon_\beta \end{bmatrix} \text{ is a conditional matrix} \tag{14}$$

Since the input matrix C is a unit matrix, it is straightforward to show that the rank of the matrix $[C \;\; CA \;\; CA^2 \;\; CA^3]^T$ equals 4. Then the system of state equations satisfies the observability. Definition of error between real value and estimated value is as follows:

$$\tilde{e}_{s\alpha} = e_{s\alpha} - \hat{e}_{s\alpha}$$
$$\tilde{e}_{s\beta} = e_{s\beta} - \hat{e}_{s\beta} \tag{15}$$

Taking dereivative of (10) - (15) yields:

$$\dot{\tilde{e}}_{s\alpha} = -\frac{1}{\varepsilon_\alpha} \tilde{e}_{s\alpha} + h_\alpha$$

$$\dot{\tilde{e}}_{s\beta} = -\frac{1}{\varepsilon_\beta} \tilde{e}_{s\beta} + h_\beta \tag{16}$$

From (10) the values $e_{s\alpha}$ and $e_{s\beta}$ are harmonic functions so exist constants $\dot{h}_{\alpha_{max}}$ and $\dot{h}_{\beta_{max}}$ such that:

$$|\dot{h}_\alpha| \le \dot{h}_{\alpha_{max}} \text{ and } |\dot{h}_\beta| \le \dot{h}_{\beta_{max}} \tag{17}$$

From [21] and (16) we have the following inequalities:

$$|\tilde{e}_{s\alpha}| \le e^{(-1/\varepsilon_\alpha)t} |\tilde{e}_{s\alpha}(0)| + \varepsilon_\alpha.\dot{h}_{\alpha_{max}}$$

$$|\tilde{e}_{s\beta}| \le e^{(-1/\varepsilon_\beta)t} |\tilde{e}_{s\beta}(0)| + \varepsilon_\beta.\dot{h}_{\beta_{max}} \tag{18}$$

Thus, if the coefficients ε_α and ε_β of the HG observer are smaller then $|\tilde{e}_{s\alpha}|$ and $|\tilde{e}_{s\beta}|$ will be bounded by smaller limits $|\tilde{e}_{s\alpha}(\infty)|$ and $|\tilde{e}_{s\beta}(\infty)|$. The smaller the values of ε_α and ε_β, are chosen, the faster the convergence of estimated values will follow the real values of $e_{s\alpha}$ and $e_{s\beta}$ of back-EMF. From the estimation of induced electromotive force, the rotor speed and position can be calculated using the following equation:

$$\hat{\theta}_e = \arctan(\frac{-\hat{e}_{s\alpha}}{\hat{e}_{s\beta}}) \tag{19}$$

$$\hat{\omega}_e = \frac{\sqrt{\hat{e}_{s\alpha}^2 + \hat{e}_{s\beta}^2}}{\lambda_m} \tag{20}$$

Or $\hat{\omega}_e = \dfrac{d\hat{\theta}}{dt}$ (21)

According to (20), the speed is plausible, but this value depends on the linkage flux, which is the quantity affected by the ambient temperature. According to (22), speed is more assured, especially in the medium and high-speed range, but is affected by process noise.

4. Simulations and results

This paper presents mixed-integer linear programming model that allows accurately and comprehensive representation the main technical and operating characteristics of thermal power units in the unit commitment problem on the spot market. Model incorporates the linear formulation of non-convex and non-differentiable variable costs, time-dependent start-up costs and inter-temporal constraints typically addressed as nonlinear. To demonstrate the system's stability and the observation capability of the HG observation set, an experiment was performed on simulation software. With the parameters of the motor include phase resistance is 2.6 Ω; the air gap between the stator and the rotor is 1 mm; the rotor mass is 0.28kg; the moment of inertia is 10.6x10-6 kgm2; the amplitude of the flux flux generated by the permanent magnet is $\lambda_m = 0.022$ Wb.

When the set speed is 4500 rpm, at the moment of 0.65 s the load torque affects the system. Figure 3 shows that the estimation speed is very fast with real speed value and the error is negligible.
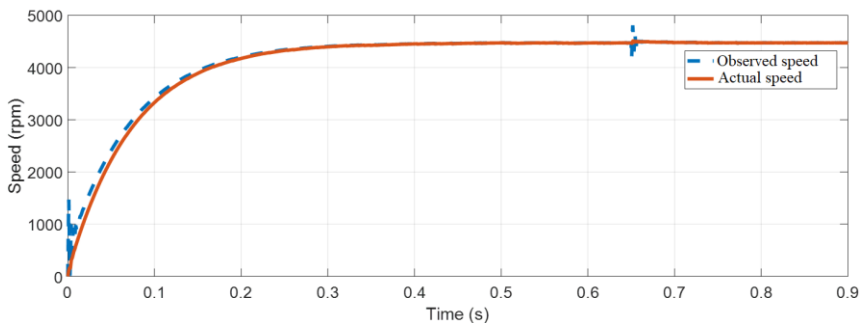

Fig. 3. Speed response under the influence of load torque

Figure 4 shows the response of the two current components i_d and i_q, where the i_q current at the beginning has a large value to accelerate the motor to quickly reach the set value, then the value drops very small at the end of the transition mode. Figure 5 shows that when the load is applied, the back-EMF component on the α axis of the observer adheres to the back-EMF component of the motor very well.
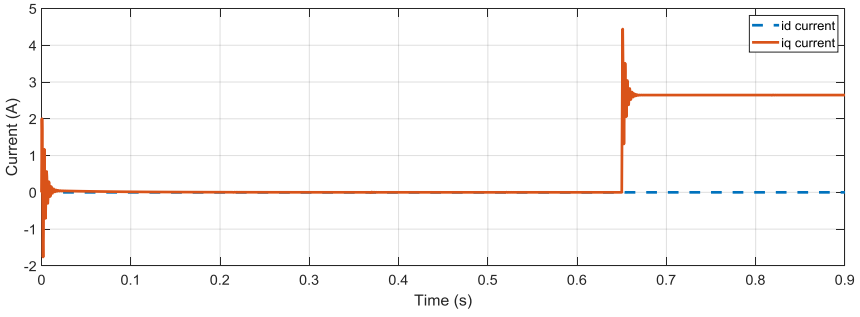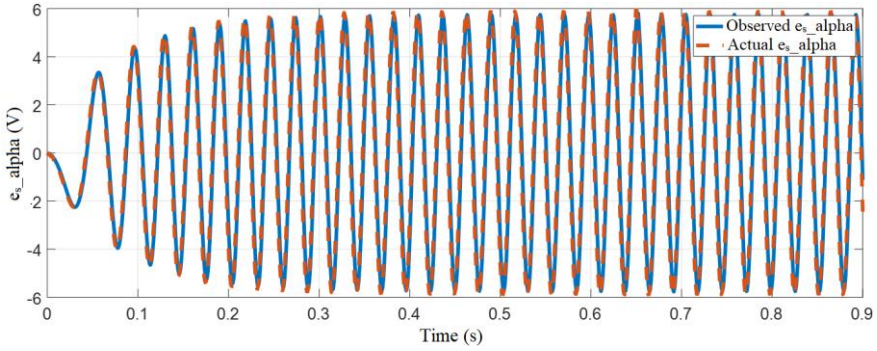
Fig. 4. Current responses i_d and i_q
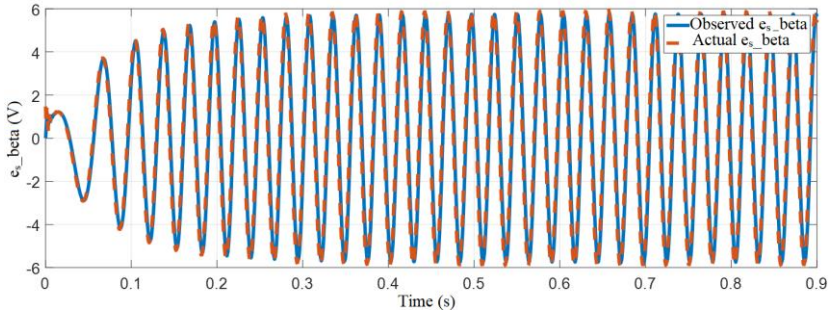

Fig. 5. Actual and observed $e_{s\alpha}$ component
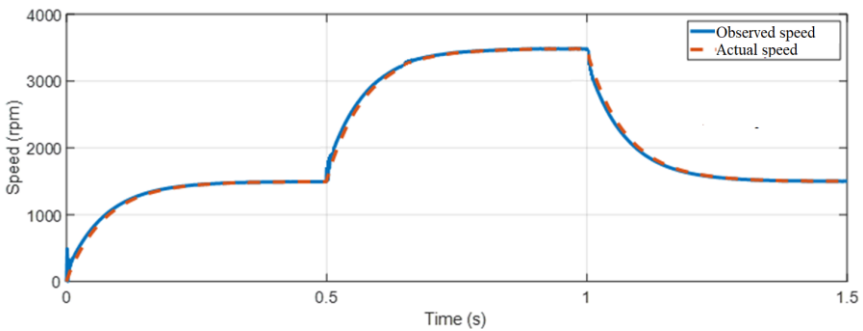

Fig. 6. Actual and observed $e_{s\beta}$ component
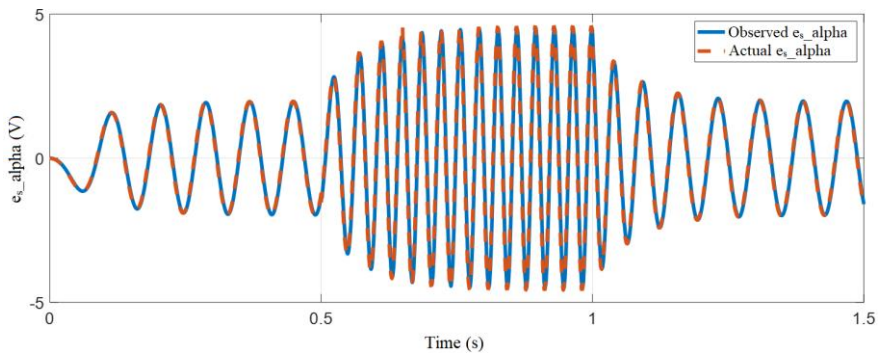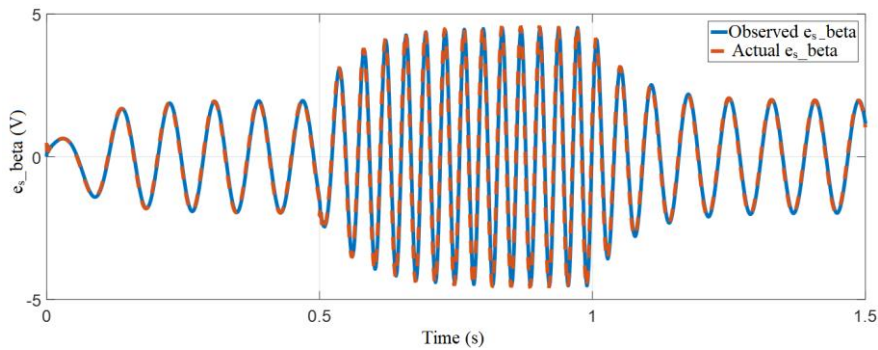

Fig. 7. Speed response

a) Response of $e_{s\alpha}$

b) Response of $e_{s\beta}$

Fig. 8. Back-EMF components on α-β coordinate

Figure 6, back-EMF components on the β axis of the observer follow the Back-EMF components of the motor very fast and few errors. Thus, in this case the HG observer estimates that the components $e_{s\alpha}$ and $e_{s\beta}$ have a sinusoidal form, with the same amplitude and following the observed value.

When changing the speed setting value from 2500 rpm- 3500 rpm- 1500 rpm we get Figure 7. Estimated speed from the observation is still capable of adhering to the speed of real value. The components $e_{s\alpha}$ and $e_{s\beta}$ at the output of the HG monitor continue to be the same sinusoidal form and follow the motor Back-EMF. Changing the speed setting value does not change the estimation time of the monitor.

5. Conclusion

The paper presented the control system without measuring a rotation speed for the synchronous motor with integrated magnetic bearing. By taking the input signal to the observer, the reference voltage and stator current, performing an estimation of the back-EMF electromotive force as the basis for calculating the position and rotor speed. The system works stably at medium speed range upwards, in which the interaction between axial position control and speed control has also been limited. However, the peak phenomenon caused by the load disturbance affects the quality of the output speed. The future work will involve in expending high-gain observer ability to deal with system external disturbances.

References

[1] D. N. Q. U. S, Salient Pole Permanent Magnet Axial-Gap Self-Bearing Motor, Magn. Bear. Theory Appl., pp. 61–83, 2010

[2] Q. D. Nguyen and S. Ueno, Analysis and control of nonsalient permanent magnet axial gap self-bearing motor, *IEEE Trans. Ind. Electron.*, vol. 58, no. 7, pp. 2644–2652, 2011, doi: 10.1109/TIE.2010.2076309.

[3] Q. Dich, Nguyen, and S. Ueno, Axial position and speed vector control of the inset permanent magnet axial gap type self bearing motor, *IEEE/ASME Int. Conf. Adv. Intell. Mechatronics, AIM*, pp. 130–135, 2009, doi: 10.1109/AIM.2009.5230025.

[4] Quang, Nguyen Phung, Dittrich, Jörg-Andreas, Vector Control of Three-Phase AC Machines, Springer, ISBN 978-3-662-46915-6

[5] Q. D. Nguyen and S. Ueno, Sensorless speed control of inset type axial gap self-bearing motor using extended EMF, 2010 *Int. Power Electron. Conf. - ECCE Asia -, IPEC* 2010, pp. 2260–2264, 2010, doi: 10.1109/IPEC.2010.5542012.

[6] D. Q. Nguyen and S. Ueno, Sensorless speed control of a permanent magnet type axial gap self-bearing motor using sliding mode observer, 2008 10th *Int. Conf. Control. Autom. Robot. Vision, ICARCV 2008*, no. December, pp. 1600–1605, 2008, doi: 10.1109/ICARCV.2008.4795764.

[7] Z. Zheng, Y. Li, F. Maurice, and X. Xiao, A rotor speed and load torque observer for PMSM based on extended Kalman filter, Proc. *IEEE Int. Conf. Ind. Technol.*, pp. 233–238, 2006, doi: 10.1109/ICIT.2006.372295.

[8] E. Robeischl, M. Schroedl, M. Krammer, Position-sensorless biaxial position control with industrial PM motor drives based on INFORM- and back EMF model, *IEEE Xplore. Restrictions apply*, February 2002, pp. 4–7.

[9] B. S. Khaldi, H. Abu-Rub, A. Iqbal, R. Kennel, M. O. Mahmoudi, and D. Boukhetala, Sensorless direct torque control of five-phase induction motor drives, *IECON Proc.* (Industrial Electron. Conf., vol. 43, no. 4, pp. 3501–3506, 2011, doi: 10.1109/IECON.2011.6119875.

[10] T. Takeshita, A. Usui, and N. Matsui, Sensorless Salient-Pole PM Synchronous Motor Drives in All Speed Ranges, *IEEJ Trans. Ind.* Appl., vol. 120, no. 2, pp. 240–247, 2000, doi: 10.1541/ieejias.120.240.

[11] S. Ichikawa, M. Tomita, S. Doki, and S. Okuma, Sensorless control of permanent-magnet synchronous motors using online parameter identification based on system identification theory, *IEEE Trans. Ind. Electron.*, vol. 53, no. 2, pp. 363–372, 2006

[12] P. D. Chandana Perera, Sensorless permanent magnet synchronous motor drives, February 2003, pp. 118-125, ISBN 87-89179-41-2.

[13] Tae-Sung Kwon, Myoung-Ho Shin, and Dong-Seok Hyun, Speed Sensorless Stator Flux-Oriented Control of Induction Motor in the Field Weakening Region Using Luenberger Observe, *IEEE Transactions on Power Electronics*, vol. 20, no. 4, July 2005

[14] Antti Piippo, Janne Salomäki, Signal Injection in Sensorless PMSM Drives Equipped With Inverter Output Filter, *IEEE Transactions on Industry Applications*, vol. 44, no. 5, September 2008

[15] Masaru Hasegawa, Satoshi Yoshioka, and Keiju Matsui, Position Sensorless Control of Interior Permanent Magnet Synchronous Motors Using Unknown Input Observer for High-Speed Drives, *IEEE Transactions on Industry Applications*,vol. 45, no. 3, May 2009

[16] S. Morimoto, K. Kawamoto, M. Sanada, and Y. Takeda, Sensorless control strategy for salient-pole PMSM based on extended EMF in rotating reference frame, *IEEE Trans. Ind.* Appl., vol. 38, no. 4, pp. 1054–1061, 2002, doi: 10.1109/TIA.2002.800777.

[17] S. Ichikawa, M. Tomita, S. Doki, and S. Okuma, Sensorless control of synchronous reluctance motors based on extended EMF models considering magnetic saturation with online parameter identification, *IEEE Trans. Ind*. Appl., vol. 42, no. 5, pp. 1264–1274, 2006.

[18] Jorge A. Solsona, María I. Valla, Disturbance and Nonlinear Luenberger Observers for Estimating Mechanical Variables in Permanent Magnet Synchronous Motors Under Mechanical Parameters Uncertainties, *IEEE Transactions on Industrial Electronic*s, vol. 50, no. 4, August 2003

[19] Huacai Lu, Ming Jiang, Xingzhong Guo and Qigong Chen, Sensorless Position Control of SPMLSM based on High-Gain Observer,,*Journal of computers*, vol. 8, no. 3, March 2013

[20] Abdullah A. Alfehaid, Elias G. Strangas, and Hassan K. Khalil, Sensorless Speed Control of PMSM Using Extended High-Gain Observers, 2019 *American Control Conference (ACC) Philadelphia*, PA, USA, July 10-12, 2019

[21] D. Won, W. Kim, D. Shin, and C. C. Chung, High-Gain Disturbance Observer-Based Backstepping Control With Output Tracking Error Constraint for Electro-Hydraulic Systems, no. m, pp. 1–9, 2014.